# AAV-Mediated *In Vivo* CAR Gene Therapy for Targeting Human T Cell Leukemia

Waqas Nawaz[1,2,3], Bilian Huang[1,2,3], Shijie Xu[1,2,3], Yanlei Li[4], Linjing Zhu[5], Zhiwei Wu[1, 2, 3*] and Xilin Wu[1, 2, 3*]

*1. Center for Public Health Research, Medical School, Nanjing University, Nanjing,*

*People's Republic of China.*

*2. State Key Laboratory of Analytical Chemistry for Life Science, Nanjing University, Nanjing,*

*People's Republic of China.*

*3. Jiangsu Key Laboratory of Molecular Medicine, Medical School, Nanjing University, Nanjing,*

*People's Republic of China.*

*4. Y-Clone Medical Science Co. Ltd. Suzhou, People's Republic of China.*

*5. Abrev Biotechnology, Nanjing, People's Republic of China.*

**Short title:** Development of off-the-shelf CAR gene therapy

**Keywords:** Adeno-associated Virus, AAV delivering CAR gene therapy, CAR-T therapy, T cell leukemia, AAV-CD4+ CAR cells, Off the shelf CAR cells development, Immunotherapy.

*Corresponding author: **Zhiwei Wu**, E-mail: wzhw@nju.edu.cn and **Xilin Wu**, E-mail: xilinwu@nju.edu.cn; Mailing address: Center for Public Health Research, Medical School, Nanjing University, 22# Hankou Road, Nanjing, Jiangsu Province, 210093, China.

Phone: 86 (25) 8368-6092. Fax: 86 (25) 8359-6023.

# Abstract

Chimeric antigen receptor (CAR) T cell therapy is the most active field in immuno-oncology and brings substantial benefit to patients with B cell malignancies. However, the complex procedure for CAR T cell generation hampers its widespread applications. Here, we describe a novel approach in which human CAR T cells can be generated within the host upon injecting an Adeno-associated virus （AAV） vector carrying the CAR gene, which we call AAV delivering CAR gene therapy (ACG). Upon single infusion into a humanized NCG tumor mouse model of human T cell leukemia, AAV generates sufficient numbers of potent *in vivo* CAR cells, resulting in tumor regression; these in vivo generated CAR cells produce antitumor immunological characteristics. This instantaneous generation of *in vivo* CAR T cells may bypass the need for patient lymphodepletion, as well as the *ex vivo* processes of traditional CAR T cell production, which may make CAR therapy simpler and less expensive. It may allow the development of intricate, individualized treatments in the form of on-demand and diverse therapies.

**Significance Statement**

AAV can generate enough CAR cells within the host. That act as a living drug, distributed throughout the body, and persist for weeks, with the ability to recognize and destroy tumor cells.

## Introduction

56   Chimeric antigen receptor (CAR) T cells have achieved significant clinical recognition with

57   remarkable responses documented for autologous CD19 (a B cell-specific antigen) redirected T

58   cells for the treatment of patients with relapsed or refractory B cell malignancies [1]. In 2017, the

59   US Food and Drug Administration (FDA) approved two autologous CD19-CAR T cell products

60   to treat certain types of relapsed or refractory large B cell lymphoma and acute lymphoblastic

61   leukemia [2]. However, CAR T cell therapy still faces skepticism and has plenty of room for

62   improvement, including challenges ranging from understanding the mechanisms and management

63   of innate and acquired resistance and cytokine release syndrome (CRS) to neurologic toxicity and

64   establishment of more efficient, less expensive, and quicker mechanisms of manufacturing [3].

65   Current clinical-scale manufacturing of T lymphocytes involves complex processes of isolation,

66   genetic modification, and selective expansion of redirected cells *ex vivo* prior to their infusion into

67   patients. This makes the manufacturing process complicated, costly and associated with clinical

68   hazards. Thus, the manufacturing of safe, affordable, easier and effective CAR T cells is critical

69   for making this therapy widely accessible for a larger population [4]. Moreover, these complicated

70   procedures are resource-intensive and require substantial technical expertise and can only be

71   performed at a limited number of specialized centers worldwide [5]. The most crucial step to

72   overcome these limitations is to create novel strategies for making this complicated and risky cell

73   therapy affordable, safer and customizable. This may in turn enable CAR T cells to outcompete

74   chemotherapy as front-line therapy.

75   Adeno-associated virus (AAV), a small, icosahedral nonenveloped virus of 25 nm in diameter

76   containing a single-stranded DNA genome, has the potential to solve this problem. AAV has

77   become an essential therapeutic gene delivery vector in recent years, it is frequently used to deliver

78 genetic material into target cells to cure or treat disease, and is extensively used in clinical

79 applications in academia and industry [6]. To date, almost 200 clinical trials using AAV have been

80 completed or are ongoing [7].

81 To manipulate immune cells *in vivo*, the carrier needs to be taken up by cells and import the

82 encoding DNA into the nucleus. Previous studies showed that AAV could transduce both dividing

83 and non-dividing cells with superior infection efficiency, which enables AAV to be widely

84 applied in gene therapy in vivo [8]. In our current study, we choose AAV-DJ (type2/type8/type9

85 chimera), which was developed by using DNA shuffling technology to produce hybrid capsids

86 from eight distinct wild-type AAV [9]. Previously, we reported AAV-DJ to deliver antibody gene

87 in vivo, where antibodies were persistent to express in cells for more than 9 weeks [10]. The

88 capability to transduce different cell types is mainly determined by the AAV capsid proteins.

89 AAV-DJ capsid was selected [9], which has higher tropism and extremely robust at transducing

90 cells [9, 11].

91 We hypothesize that human CAR T cells can be generated to specifically kill target cells within

92 the host upon injecting an AAV vector carrying the CAR gene, which we call AAV delivering

93 CAR gene therapy (ACG). To prove this concept, we furnished an AAV vector with plasmid DNA

94 encoding a CD4-CAR, which is composed of a single-chain antibody (scFv) specific for the

95 extracellular domain of the CD4 antigen fused with CD28, 4-1BB, and CD3 zeta cytoplasmic

96 signaling domains. We demonstrated that the modified AAV vector could safely deliver the CAR

97 gene into the host cells of humanized NCG (NCG-HuPBL) mice and reprogrammed cells to

98 express the CAR. As envisioned, the AAV vector generated enough CAR T cells *in vivo* and thus

99 caused effective tumor regression and produced antitumor immunological characteristics. In

100 addition, *ex vivo* experiments indicated that our AAV delivering the CD4-CAR potently eliminated

4

101 tumor cells from adult T cell leukemia (ATL). The current approach may skip the technically

102 challenging *ex vivo* procedures and enable the host to create its CAR T cells.

103

## Methods and materials

### Mice

106 NCG mice were purchased from GemPharmaTech. NCG mice were maintained in accordance

107 with the Guide for the Care and Use of Laboratory Animals of the Medical School of Nanjing

108 University. All experiments were performed according to the guidelines of the Institutional Animal

109 Committee of Nanjing University.

### PBMCs and cell lines

111 Peripheral blood mononuclear cells (PBMCs) (derived from healthy donors visiting the Drum

112 Tower Hospital, Nanjing University) were isolated from buffy coats by Ficoll-Hypaque gradient

113 separation, and cultured in RPMI-1640, 10% heat-inactivated FBS and freshly added recombinant

114 human interleukin-2. Excess PBMCs were cryopreserved until use. For stimulation, PBMCs were

115 washed once in T cell medium without IL-2 and then suspended at a concentration of $10^6$/ml in T

116 cell medium containing IL-2 (300 IU/ml) and anti-human CD3 antibody (1 μg/ml). Cells were

117 incubated in 5% $CO_2$ at 37°C for 2 days until AAV transduction.

118 AAV-293T (Thermo Fisher) and HEK-293T (ATCC) cells were maintained in Dulbecco's

119 modified Eagle medium (DMEM) containing 10% FBS and 2 mM glutamate. H929, MT2, and

120 Jurkat cell lines (ATCC) were grown in RPMI-1640 with 10% heat-inactivated FBS. CD4

121 expression was authenticated by flow cytometry in MT2 and Jurkat cell lines prior to experiments.

122 All cell culture media contained 100 U/ml penicillin-streptomycin (Gibco, Invitrogen). All cell

123 lines were maintained in an environment of 37°C and 5% $CO_2$.

5

124 **Construction of AAV-CAR vectors**

125 A recombinant AAV-2 ITR-containing plasmid (pAAV-MCS) with an expression cassette

126 containing inverted terminal repeats was used for AAV generation. To generate AAV-CD20CAR

127 and AAV-CD4CAR, we used the sequence of CD20-binding scFv from NCBI (GenBank,

128 KM043780) and the sequence of Hu5A8 specific for the CD4 backbone with a 20-mer (Gly4Ser)

129 adopted from our previous study [10]. The scFv was fused with CD28 hinge-transmembrane

130 regions linked to 4-1BB (CD137) intracellular domains and the CD3 zeta intracellular domain

131 [12]. CAR DNA (Hu5A8-CD28-41BB-CD3 or Rit-CD28-41BB-CD3) was cloned into the

132 ITR/MCS-containing vector. Plasmid sequence and construction were confirmed by sequence

133 analysis and restriction enzymes. Stocks of pAAV-Hu5A8-CD28-41BB-CD3 and pAAV-Rit-

134 CD28-41BB-CD3 were prepared as pAAV vectors of interest (VOIs).

135 **AAV production**

136 AAV of DJ subtype was prepared by polyethyleneimine (PEI)-based triple transfections of pAAV-

137 VOI, pHelper (helper plasmid) and pAAV-DJ (catalog number VPK-430-DJ, Cell Biolabs), as

138 described [13]. Briefly, the medium of 80–90% confluent AAV-293T cells in 15 cm plates was

139 changed to fresh DMEM 2 hours before transfection. Plasmids at a ratio of 1:1:1 (25 µg each

140 plasmid for a 15 cm plate) were mixed with 2 ml Opti-MEM in a 15 ml tube. Three hundred

141 microliters of PEI (Polysciences Inc.) (1 mg/ml) was added to 2 ml Opti-MEM in another 15 ml

142 tube and was mixed by vortexing and incubated for 15 min at room temperature, after which the

143 mixture was gently added to the serum-free medium in the plate and incubated in a standard 5%

144 $CO_2$ and 37°C incubator. The supernatant was collected 24, 48, 72, and 96 hours posttransfection,

145 and the debris was cleared by centrifugation and filtration (0.45 µM). AAV was concentrated by

146 centrifuging (1000g for 5min) with 10% polyethylene glycol 8000 and 14% 4 M NaCl (by volume)

6

147    and incubated overnight at 4°C. The next morning, the sample was transferred to 50 ml conical

148    tubes and centrifuged at 4000 g for 30 min at 4°C. The AAV pellet was resuspended in PBS and

149    stored at -80°C. We used qPCR to determine the number of genome-containing particles in an

150    AAV prep using SYBR green technology, adopted from our previously reported protocol [10].

151    The detailed procedure of determining the genome-containing particles in an AAV prep using

152    SYBR green technology is explained in the supplementary information.


153    **AAV transduction of HEK-293T and T cells.**

154    Three different doses of AAVs were administered: $1 \times 10^4$ AAVs/cell was considered AAV low

155    (L), $1.5 \times 10^4$ AAVs/cell was considered AAV middle (M), and $1 \times 10^5$ AAVs/cell was considered

156    AAV high (H). The day before transduction, HEK-293T cells were trypsinized and counted, and

157    $1\text{-}4 \times 10^5$ cells were plated in 2.0-3.0 ml complete culture medium and incubated at 37°C overnight.

158    Sixteen hours later, purified AAV (AAV-CD4CAR or AAV-CD20CAR) was added to each well

159    at different doses by gentle swirling/mixing. Twenty-four hours post-transduction, fresh media

160    containing 20% FBS was added, and the cells were cultured for 2-3 days and then analyzed by

161    FACS, or fluorescence microscopy.

162    The T cells were activated and infected with AAV-CAR as described [14]. Briefly, $10^6$ cells were

163    plated on day 0 and activated for two days in the presence of 300 IU/ml IL-2 and 1 μg/ml anti-

164    human CD3 antibody. On day 2, purified AAV (AAV-CD4CAR or AAV-CD20CAR) was added

165    to each well at different doses by gentle swirling/mixing and incubated at 37°C in the presence of

166    5% $CO_2$. The next morning following transduction, fresh media containing 20% FBS was added,

167    and the cells were cultured for 2-3 days and then analyzed by FACS or florescence microscopy.

**Flow cytometry**

All antibodies for flow cytometry were purchased from BioLegend or Invitrogen. Cells were stained with target antibodies (according to the experiment's requirement), whereas for CAR expression, target antigen (CD4Fc protein) was used. After 30 minutes at 4°C, cells were washed once, suspended in FACs buffer, and stained with Alexa flour488 anti-rabbit for 30 minutes at 4°C. For in vivo samples, cells were lysed by RBC lysis buffer (BD), by incubating the cells with 1X lysis buffer at room temperature for 10 minutes. Labeled cells were washed twice and suspended in FACs buffer. All cells were measured and sorted by using a NovoCyte FACS, and analyzed with FlowJo software version 10.2.

**CAR T cell-mediated cytotoxicity assay using CFSE and 7-AAD**

Cytotoxicity assays were carried out using CFSE and 7-AAD, as previously described [15]. Briefly, CFSE-labeled target cells were incubated with different doses of AAV-CD4CAR- and AAV-CD20CAR-infected PBMCs for 24 hrs at 37°C. After 24 hours of incubation, 7-amino-actinomycin D (7-AAD; BD Pharmingen) was added, as recommended by the manufacturer. The fluorescence was analyzed by flow cytometry. Target cell cytotoxicity was calculated using the following formula: cytotoxicity = 100 x [(CFSE-labeled dead target cells)/ (CFSE-labeled dead target cells + CFSE-labeled lived target cells)].

***In vivo* NCG-HuPBL mouse model for the *in vivo* CD3+CD4+ depletion assay**

NCG mice were purchased from GemPharmaTech. NCG mice were maintained in accordance with the Guide for the Care and Use of Laboratory Animals of the Medical School of Nanjing University. All experiments were performed according to the guidelines of the Institutional Animal Committee of Nanjing University. The humanized NCG (NCG-HuPBL) mouse model was developed as reported previously by our group [16]. Briefly, human PBMCs were obtained from

191    healthy individuals' peripheral venous blood and purified by Ficoll-Paque (Pharmacia, Piscataway,

192    NJ) density gradient centrifugation as described above in detail. Freshly isolated PBMCs were

193    resuspended in PBS, and $1.5 \times 10^7$ PBMCs/mouse were injected intraperitoneally into NCG mice.

194    PBMC engraftment was confirmed after 3 weeks by FACS, and mice with an appropriate percent

195    ratio of CD3+CD4+ and CD3+CD8+ were considered successful NCG-HuPBL mouse models. A

196    total of $5 \times 10^6$ *ex vivo*-transduced AAV-CD4CAR T cells or $1 \times 10^{11}$ AAV-CD4CAR T cells and

197    $1 \times 10^{11}$ AAV-CD20CAR T cells were injected into each Hu-NCG mouse according to the specified

198    grouping. Mice were bled via the submandibular vein, and peripheral blood cell populations and

199    CAR expression were analyzed periodically using flow cytometry.

200    ***In vivo* NCG-HuPBL tumor mouse model**

201    After successfully engrafting PBMCs in NCG mice, we modeled T cell tumors by intraperitoneally

202    injecting $2.5 \times 10^6$ luciferase-expressing MT2 cells into each NCG-HuPBL mouse (generation of

203    stable luciferase-expressing MT2 ATL tumor cell line is explained in Supplementary information).

204    NCG-HuPBL mice injected with luciferase-expressing MT2 cells underwent *in vivo*

205    bioluminescence imaging at various times as specified for each experiment. Luciferase-based

206    bioluminescence imaging was performed with a NightOWL II LB 983 (Berthold) *in vivo* imaging

207    system. Mice were first anesthetized by inhaling isoflurane and were maintained with 2%

208    isoflurane during imaging procedures. Mice were injected (I.P.) with D-luciferin (prepared in

209    DPBS) at 150 mg/kg and imaged immediately after anesthesia. Images were captured, and

210    bioluminescence intensity and tumor area were quantitated using Indigo live imaging analysis

211    (Berthold). Total flux and area were measured through the automated analysis method by Indigo

212    (Berthold).

**Confocal microscopy**

213

214    Samples from mice for confocal imaging were prepared as described previously [17]. Briefly, cells

215    were stained for CD4-Fc protein and with an anti-CD45^{+} antibody for 1 hour. Next, the cells were

216    washed and stained with anti-CD4-Fc secondary antibody for 1 hour. Following washing, the cells

217    were transferred onto a fibronectin matrix (Sigma Aldrich) and fixed in 2% paraformaldehyde.

218    Slides were mounted with #1.5 coverslips and Mowiol mounting medium and examined using an

219    FV3000 confocal microscope.

220    *In vivo* **cytokine measurement**

221    *In vivo* cytokines from the serum/plasma of mice were measured using the Cytometric Bead Array

222    Human Th1/Th2 Cytokine Kit (BD), following the manufacturer's instruction. The kit was used

223    for the simultaneous detection of Human TNF, IL-2, IL-6, IL-4, and IL-10 in a single sample. The

224    Cytometric Bead Array Human Th1/Th2 Cytokine Kit contains a mixture of various capture beads

225    with different fluorescent intensities which are coated with capture antibodies specific for each

226    cytokine. First, we mixed the beads coated with six specific capture antibodies. Next, 50 μL of the

227    mixed captured beads, 50 μL of phycoerythrin (PE) detection reagent, and 50 μL of the unknown

228    serum sample or standard dilutions were added sequentially to each assay tube and incubated for

229    2 h at room temperature in the dark. The samples were washed with 500 μL of wash buffer and

230    centrifuged at 800g for 5 mint. The bead pellet was resuspended in 400 μL buffer after discarding

231    the supernatant. All the samples were sorted on the NovoCyte FACS. Fluorescent intensities give

232    the individual cytokine concentration. The standard curve for the CBA assay was determined using

233    different dilutions. The data were analyzed with FCAP Array software provided by BD.

234

235    **Statistical analysis**

10

236    Specific statistical tests and metrics (median, mean, standard error) used for comparisons, along

237    with sample sizes, are described in the Results and Figure legends. All statistical analyses were

238    performed using GraphPad Prism software version 6.0. ns, no significance; ****$P < 0.0001$; ***,

239    $P < 0.001$; **, $P < 0.01$; *, $P < 0.05$.

240

## Results

242    **Design and characterization of AAV-CD4CAR**

243

244    As schematically shown in Figure 1a, AAV-CD4CAR is the third-generation CAR construct

245    composed of anti-CD4 scFv, hinge (H) and transmembrane regions, and CD28 and 4-1BB

246    intracellular signaling domains in tandem with the CD3 zeta signaling domain. The CD4-CAR

247    DNA molecule was subcloned into the pAAV-VOI plasmid, which was mixed with the plasmids

248    pAAV-Helper and pAAV-DJ to generate AAV virus carrying the CD4-CAR gene (AAV-

249    CD4CAR). To verify the AAV-CD4CAR construct, infected HEK-293T cells were subjected to

250    Western blot and fluorescence-activated cell sorting (FACS) analysis. Immunoblotting with an

251    anti-CD3 zeta monoclonal antibody showed bands of the expected size for the AAV-CD4CAR

252    CD3 zeta fusion protein, while the control cells infected with AAV-GFP showed no bands (Fig.

253    1b). Furthermore, AAV-CD4CAR infection efficiency was analyzed through FACS using CD4-

254    Fc protein (Fig. 1c). Moreover, AAV-CD4CAR infects cells with limited toxicity and high

255    viability (Supplementary Fig. 1a-c).

256    We characterized the effect of AAV-CD4CAR on T cells from healthy donors. Human T cells

257    were activated with IL-2 and anti-human CD3 antibody and then infected with different doses of

258    AAV-CD4CAR (MOI $1 \times 10^4$, $0.5 \times 10^5$, and $1 \times 10^5$). As expected, a dose-dependent expression

259    of the CD4-CAR on T cells was observed (Figure 1d). We found that AAV-CD4CAR induced

11

260 dose-dependent expression in three different healthy donor samples. However, the percentage of

261 expression varied among donors, but the difference was not statistically significant

262 (Supplementary Figure 2a). Upon more detailed phenotyping, we found that CD4+ T cells also

263 expressed AAV-CD4CAR but at a significantly lower rate than CD8+ T cells (Supplementary

264 Figure 2b).

265 In summary, these results confirmed that our AAV-CD4CAR contain the CD3 zeta on the

266 intracellular end and the anti-CD4 scFv on the extracellular end, verifying that all other elements

267 were present. Furthermore, AAV-CD4CAR infect the T cells and produce AAV-CD4CAR T cells

268 in a dose-dependent manner.

269 **AAV-CD4CART cells are CD4 specific and eliminate leukemic cells *in vitro* and aggressive**
270 **CD4$^+$ ATL cells *ex vivo***

271 We furnished our AAV-CD4CAR with the scFv region of the Hu5A8 antibody specific for CD4,

272 which we reported previously for HIV treatment [10]. We next evaluated the functional ability of

273 AAV-CD4CAR to eliminate CD4$^+$ cells in PBMCs from various donors (n=10) during T cell

274 expansion following AAV-CD4CAR transduction. As expected, the groups treated with AAV-

275 CD4CAR had a decreased CD3$^+$CD4$^+$ T cell subset within 2-3 days following AAV-CD4CAR

276 transduction in a dose-dependent manner compared to the vector control group (Figure. 2b).

277
278 AAV-CD4CAR was tested *in vitro* for its antileukemic activity using CD4-positive MT2 and

279 Jurkat cells as targets. In addition, the CD4-negative cell lines H929 and AAV-CD20CAR served

280 as a negative control. The MT2 cell line is an adult T cell leukemia (ATL) cell line with aberrant

281 CD4 expression established by co-culture of normal human cord leukocytes with leukemic cells

282 from ATL patients [18]. Jurkat cells are immortalized T lymphocytes obtained from a patient with

283 T cell leukemia [19]. CD4 expression on MT2 and Jurkat cells was counterchecked by flow

284    cytometry prior to experiments. H929 is a B cell line with CD38 expression established from a

285    malignant effusion in a patient with myeloma [20]. 48 hours after co-culture with human PBMCs

286    infected with various doses of AAV-CD4CAR, MT2, and Jurkat cells were effectively lysed in a

287    dose-dependent manner. However, neither the CD4$^-$ cell line (H929) nor the MT2 cells treated

288    with a CD20-CAR were lysed (Figure. 2c). Next, we performed an *ex vivo* experiment to evaluate

289    the ability of AAV-CD4CAR to kill primary ATL cells. CD3$^+$CD4$^+$ primary cells from an

290    unclassified and chemotherapy-resistant ATL patient were isolated *ex vivo* and served as a target

291    population. CD3$^+$CD4$^+$ ATL cells were completely lysed (depleted to ∼ 0%) by AAV-CD4CAR

292    48 hours post-infection, while AAV-CD20CAR was unable to lyse CD3$^+$CD4$^+$ ATL cells (Figure.

293    2d). In summary, these results show that AAV-CD4CAR-infected cells exhibited dose-dependent,

294    profound, and specific antitumor activity against T cell leukemia cell lines. Similarly, they could

295    also completely lyse the tumorigenic CD3$^+$CD4$^+$ population in samples from ATL patients in *ex*

296    *vivo* coculture. Altogether, these results signify that AAV-CD4CAR-infected cells are specific for

297    CD4$^+$ cells.

298    **CAR T cells generated from in vivo reprogramming of lymphocytes via AAV and their**

299    **antitumor immunological characteristics**

300    We hypothesized that our AAV carrying CAR gene construct could reprogram lymphocytes and

301    are able to generate *in vivo* CAR T cells to kill target cells in a process that we called ACG. To

302    experimentally prove our ACG concept, we transplanted human PBMCs into NCG mice, and after

303    successful engraftment of PBMCs, we injected 1 x 10$^{11}$ AAV-CD4CAR into NCG-HuPBL mice.

304    Interestingly, FACS analysis of blood collected after 48 hours showed that the AAVs started

305    infecting the immune cells, and 9% of CD45$^+$ cells expressed the CD4-CAR (Figure. 3a). We

306     further confirmed CD4-CAR expression on CD45$^+$ cells through confocal microscopy. Infused

307     AAV-CD4CAR were taken up by lymphocytes, and the CD4-CAR could be observed on the

308     lymphocyte membrane (Figure. 3a).

309     CAR T cells combine features of cell therapy, gene therapy, and immunotherapy. Antitumor

310     characteristics, including transduction efficiency, transgene expression levels, stability or

311     retention, cytokine production, are all key to these processes. Next, we evaluated the stability and

312     biodistribution of AAV-CD4CAR T cells in NCG-HuPBL mice. Our results showed that the

313     AAVs efficiently delivered CD4-CAR DNA into host CD3$^+$CD8$^+$ T cells, which resulted in the

314     production of enough CD4-CAR T cells, which circulate in the host body for weeks (Figure. 3b).

315     We quantified the biodistribution of AAV-CD4CAR T cells in different organs after injecting

316     AAV-CD4CAR into NCG-HuPBL mice. AAV-CD4CAR T cells were distributed in various

317     organs, with the highest concentrations in the spleen and blood (Figure. 3c). Cytokine production

318     is a hallmark of CAR T cell therapy; therefore, we assessed cytokine production in an ATL NCG-

319     HuPBL mouse model. Our results showed that *in vivo*-generated AAV-CD4CAR cells were

320     robustly functional against tumor cells and were able to produce a series of cytokines (Figure. 3d).

321     Taken together, the findings from these experiments suggest that an AAV encoding a CAR gene

322     can reprogram sufficient immune effector cells to generate *in vivo* CAR T cells. Furthermore, the

323     *in vivo*-generated AAV-CD4CAR T cells can circulate in the host body for weeks and induce

324     antitumor immunological characteristics. These results indicate that the ACG strategy can generate

325     CAR T cells *in vivo.*

**Functional characterization of *in vivo*-generated AAV-CD4CAR T cells**

327     Encouraged by the expression and antitumor immunological characteristics of *in vivo*-generated

328     AAV-CD4CAR T cells, we next decided to compare the functional ability by comparing the

14

329    $CD3^+CD4^+$ cell depletion and CAR expression of *in vivo*-generated AAV-CD4CAR T cells with

330    those of conventional CAR T cells. We prepared NCG-HuPBL mice transplanted with PBMCs

331    (Figure. 4a) and divided them into four groups: PBS group (untreated control), AAV-CD20CAR

332    group (negative control), AAV-CD4CAR T cell group (positive control), and AAV-CD4CAR

333    group (treatment group). Prior to any treatment, NCG-HuPBL mice were randomly divided into

334    each group with no significant difference in $CD3^+CD4^+$ percentage at day 0 (Supplementary

335    Figure. 3a). We treated the positive control mice with six million T cells infected *in vitro* with

336    AAV-CD4CAR. This amount corresponds to the approved high dose of CAR T cells currently

337    being used in clinics, in which patients are administered $2 \times 10^6$ CAR T cells/kg of mean body

338    weight [21]. However, we infused a single dose of $1 \times 10^{11}$ AAV into the treatment group (AAV-

339    CD4CAR) and a negative control group (AAV-CD20CAR). As envisioned, a single dose of AAV

340    $(1 \times 10^{11})$ infusion was able to yield enough AAV-CD4CAR T cells *in vivo,* similar to the number

341    of *ex vivo* transduced cells after infusion (Figure. 3b and 3c). Correspondingly, $CD3^+CD4^+$ cells

342    started decreasing within the first week in the positive control and treatment groups. After two

343    weeks, there was a significant difference in $CD3^+CD4^+$ cell percentage between the positive

344    control and treatment group compared to the negative control and untreated mice (Figure. 4d).

345    However, there was no difference observed between the positive control and the treatment group,

346    suggesting that the targeting potential of the *in vivo*-generated AAV-CD4CAR T cells was similar

347    to that of the conventional CAR T cells. Similarly, no significant difference was observed in

348    percent survival between the positive control mice and the treatment group (Figure. 4e). In

349    summary, the above results show that *in vivo*-generated AAV-CD4CAR T cells are functionally

350    potent and effective against the target in NCG-HuPBL mice and have similar efficiency to that of

351    conventionally manufactured CAR T cells.

15

352    Next, we also evaluated the relative effects of the ACG approach on blood count, serum chemistry,

353    and mean body. We calculated the bodyweight at different time intervals and collected blood for

354    complete blood count (CBC) and serum chemistry. There was no difference in the mean body

355    weight between the *in vivo*-generated AAV-CD4CAR T group and the untreated group

356    (Supplementary Figure. 3b). Furthermore, serum chemistry and complete blood count values were

357    normal and almost similar to those of the untreated mice (Supplementary Figure. 3c, d). The slight

358    difference in the AAV treated group compared to the PBS group may be due to cytokines

359    production in AAV treated groups. In summary, these results suggesting the safety of the ACG

360    approach for the generation of *in vivo* CAR T cells.

361    ***In vivo* antitumor activity of ACG**

362    We further assessed whether the *in vivo*-generated AAV-CD4CAR T cells could eradicate the

363    tumor in NCG-HuPBL mice. To establish a tumor-bearing NCG-HuPBL mouse model, we first

364    injected PBMCs into NCG mice and selected successful PBMC-engrafted NCG-HuPBL mice,

365    followed by intraperitoneal injection of luciferase-expressing MT2 ATL cells to develop an ATL

366    NCG-HuPBL mouse model. Mice were randomly divided into two groups: the untreated group

367    (PBS) and the treated group (AAV-CD4CAR). Two days after establishing the ATL NCG-HuPBL

368    mouse model, we injected $2 \times 10^{11}$ AAVs carrying the CD4-CAR gene into the treatment group

369    (Figure. 5a). Interestingly, the ACG strategy started causing tumor reduction at day 10, which

370    became more apparent at day 17 and day 25 (Figure. 5b, c). The mean tumor area of AAV-

371    CD4CAR-treated mice was significantly reduced compared with that of the untreated group

372    (Figure. 5d). Four out of six mice in the treated group presented complete tumor remission. One

373    mouse (M10) showed tumor recurrence when analyzed at day 25 (Figure. 5b). In the untreated

374    group, none of the mice showed any regression in tumor burden, suggesting stable tumor growth

375    over time (Figure. 5b). As $CD45^+CD4^+$ cells are present in both healthy PBMCs and MT2 ATL

376    cells, we next analyzed the $CD45^+CD4^+$ population in mice at the end of the study (day 25) to

377    evaluate the tumor burden at the cellular level. Our results showed that the percentage of

378    $CD45^+CD4^+$ cells in the untreated NCG-HuPBL ATL mice was higher than that in the untreated

379    NCG-HuPBL mice (NCG mice engrafted with PBMCs only, no tumor) (Figure. 5e). This higher

380    percentage of $CD45^+CD4^+$ cells was due to the injected tumor cells that expressed $CD4^+$ cells.

381    Interestingly, the FACS results also showed that the $CD45^+CD4^+$ cells were completely depleted

382    in the ACG-treated mice, while no depletion was observed in the untreated mice (Figure. 5f).

383    Furthermore, a significant percentage of $CD3^+CD8^+$ cells showed AAV-CD4CAR expression in

384    the treated group (Figure. 5f). The $CD45^+CD4^+$ depletion and CAR expression in the $CD3^+CD8^+$

385    population agreed with the tumor burden analyzed by IVIS signal and tumor size in each mouse

386    (Supplementary Figure. 4 a, b). Next, we evaluated the tumor burden at the organelle level. Two

387    mice from each group were euthanized at the end of the study, dissected, and analyzed for IVIS

388    signals (Supplementary Figure. 4 c). Tumors were almost completely eradicated from all organs

389    in AAV-CD4CAR-treated mice, except in one mouse (M10), which showed a small tumor burden

390    in the intestinal region (the same mouse that had tumor recurrence). However, a significant amount

391    of tumor was observed in all the organs in the untreated mice (Figure. 5g). In summary, our results

392    showed that when an AAV carrying the CD4-CAR gene was infused into mice, it could quickly

393    reprogram lymphocytes and generate sufficient CAR cells to induce ATL regression in NCG-

394    HuPBL mice, suggesting that ACG could be a potential strategy for tumor treatment.

395

396

397

## Discussion

398

399

400 AAV has been intensively investigated for gene therapy in preclinical and clinical studies. AAV

401 vectors are among the most suitable tools for *in vivo* gene delivery due to their superior

402 infection efficiency and unique biological and biophysical properties [22]. AAV shows persistent

403 transgene expression and long-term correction of disease phenotype with little or no toxicity in

404 clinical and preclinical studies [23]. In our current study, we used AAV equipped with a

405 synthetic gene to manipulate immune cells. To the best of our knowledge, this is the first report

406 describing that an AAV carrying a CAR gene can reprogram immune cells *in vivo* to generate

407 enough CAR T cells to induce tumor regression. Our current CAR gene-carrying AAV strategy

408 contrasts with the costly and time-consuming method of conventional manufacturing CAR T

409 therapy, which requires primary T cell isolation and transgene introduction and expansion via

410 lentiviral vectors or retroviral vectors *ex vivo*.

411 We used humanized NCG-HuPBL mice throughout our study, which not only recapitulate ATL

412 but also other antitumor immunological characteristics [24]. In our current study, we chose CD4-

413 targeting CAR transgenes because $CD4^+$ leukemia and lymphoma are highly aggressive types of

414 tumors that are extremely refractory to chemotherapy. Initial preclinical studies of CAR T cells

415 for targeting $CD4^+$ tumors are encouraging, but to date, no standard care has been developed [25].

416 Furthermore, CD4+ cells are the major latent reservoir of HIV, posing a challenge for HIV

417 eradication; therapies targeting $CD4^+$ cells can also be translated into HIV treatment [26] and

418 treatments for other infectious diseases, including systemic lupus erythematosus, rheumatoid

419 arthritis, multiple sclerosis and psoriasis [27-30]. Previously, our group tested the same targeting

420 antibody (Hu5A8) in humanized NSG-HuPBL mice for HIV treatment [10].

18

421 An interesting outcome of our study was that AAVs are capable of producing enough *in vivo* CAR

422 T cells upon a single infusion, and these T cells are potent as *ex vivo*-generated CAR T cells.

423 Furthermore, once produced, they act as a living drug, are distributed throughout the host, and

424 circulate in the host body for weeks, with the ability to recognize and destroy target cells.

425 Conventional lentivirally or retrovirally transduced cells tend to lose their transgenes expression

426 over time [31]. AAV vectors lack engineered lipids and chemical components and are free from

427 viral genes, and thus considered to be safe for gene therapy with limited toxicity [32]. In general,

428 AAV has been reported to be less immunogenic than other viruses and synthetic carriers.

429 The complete $CD4^+$ depletion in NCG-HuPBL mice raises concern for adverse effects in the long

430 term or clinical setting. CD4 helper T cell depletion for long periods leads to "on-target, off-tumor"

431 toxicities and immunodeficiency in patients [33]. Furthermore, the persistence and production of

432 memory AAV-CD4CAR T cells may further extend CD4 cell aplasia in the clinical setting, thereby

433 suggesting the need for a safety switch. One such approach is to eliminate CAR T cells completely

434 from the host. Ma et al. [34] used alemtuzumab (anti-CD52 antibody), which resulted in

435 eliminating CAR T cells within a few hours. Furthermore, such a situation can also be tackled in

436 advance by integrating recently documented multiple advanced logic and control features for CAR

437 T cells [35, 36] into our ACG system.

438 CAR T cells have emerged as a promising therapy for the treatment of various tumors during the

439 last few years and have obtained approval from the FDA to treat large B cell lymphomas such as

440 non-Hodgkin lymphoma and B cell ALL [1]. Currently, multiple clinical trials and preclinical

441 studies are ongoing to expand the therapeutic applications of CAR T cells. As mentioned earlier,

442 CAR T cell production is a multiplex system involving cell therapy, gene therapy, and

443 immunotherapy. This multiplex system of CAR T cell production limits the therapeutic potential

19

444    of CAR T cells to a few tumor types and specialized centers around the globe [37]. Several

445    strategies are currently being developed to generate allogenic CAR T cells, including genome

446    editing of T cells [38], *in vivo* engineering of T cells relying on the infusion of nanoparticles [39],

447    and strategies involving lentivirus [40], using alternative effector cells (NK cells, γδ T cells, and

448    macrophages) [41, 42], donor-derived allogeneic CAR T cells [43], and nonalloreactive T cells

449    [44] as well as the split, universal, and programmable CAR system (SUPRA) [35]. All these

450    approaches bear advantages and disadvantages [45]; however, we believe that the AAV-based *in*

451    *vivo* approach may be simpler to operate in a clinical setting since it transduces dividing and

452    nondividing cells without requiring a strong T cell activation signal. Unlike, Lentivirus and

453    synthetic vector, AAV DNA can persist in episomal form and used host endoplasmic reticulum

454    for uncoating. The episomal form of the AAV DNA is very stable and cannot be degraded by

455    exonucleases [46], thus making it a suitable carrier for manipulating in vivo cells. Additionally,

456    ample evidence from various AAV-based clinical studies has shown the safety of AAVs delivering

457    genes [47].

458    Our ACG strategy involving *in vivo* generation of CAR T cells has the potential to overcome the

459    abovementioned hurdles and will make CAR T cell treatment easier and affordable, and will

460    transform an intricate, individualized treatment into a broadly applicable product. AAV-DJ

461    subtype for manipulating in vivo immune cells exhibits higher transduction efficiency and broader

462    tropism [11, 48]. Therefore, upon infusion in humanized mice, AAV-CD4 CAR based on AAV-

463    DJ subtype might infect numerous host and target cells. However, the current study aims to give a

464    proof of concept of the ACG method; thus, we evaluate the in vivo generation and properties of

465    key effector cells for CAR therapy, i.e., T cells. Despite our strong proof-of-concept of ACG, there

466    are still many concerns and limitations in our current study, which need to be addressed in the

467    preclinical setting to make these *in vivo*-generated AAV-CAR T cells as effective and safe as *ex*

468    *vivo*-generated CAR T cells. One major limitation of the current study is the specificity of AAV

469    carrying the CAR gene, and we did not evaluate the CAR expression in hematopoietic cells, tumor

470    cells, and other immune cells. Furthermore, the current study is the lack of having strong data to

471    evaluate the biocompatibility and safety of the ACG approach, and the Hu-PBL NCG may not

472    fully recapitulate the human immune microenvironment. Further studies will be required to design

473    an ACG with ligand coupling or modification in the AAV capsid for cell-specific delivery of the

474    CAR gene. Additionally, a deep insight into its biocompatibility and safety in larger and versatile

475    animal models, and evaluating its therapeutic potential in other tumor models will facilitate clinical

476    translation of this approach. In addition to the in vivo CAR T cells generation, given further

477    optimization, our ACG strategy may lay the foundation for *in vivo* T cell manipulation in

478    immunotherapy beyond cancer and infectious diseases. We believe that the ACG strategy will

479    substantially streamline the manufacturing process of cell-based therapies in the clinical setting

480    and will make genetically engineered cell treatment less expensive and more effective.

481

482    **Conflict of interest**

483
484    The patent (CN201910224056.8) was filed by Xilin Wu, Zhiwei Wu and Waqas Nawaz as

485    inventors of the AAV *in vivo*-generated CAR cell concept. All other authors declare that they

486    have no conflicts of interest.

487    **Findings**

488

492     Ningxia University Collaborative Project (grant #2017BN04), Jiangsu Province

493     "Innovative and Entrepreneurial Talent" project and Six Talent Peaks Project of Jiangsu Province.

494

495     **Data availability**

496     Plasmids generated in this study will be made available upon reasonable request from the

497     corresponding author. Detailed methods, materials, and troubleshooting strategies are provided as

498     Supplementary Information.

499

500     **Ethics**

501     The study and the protocol for this research were approved by the Center for Public Health

502     Research, Medical School, Nanjing University. All experimental animal procedures were

503     approved by the Committee on the Use of Live Animals by the Ethics Committee of Nanjing Drum

504     Tower Hospital. All the authors declare their compliance with publishing ethics.

505

506     **Author contribution**

507     All authors contributed to the work fulfilling the criteria adopted from ICMJE. Acquisition of data:

508     WN, WX, BH, SX, ZR, ZL, and YL. Analysis and interpretation of data: WN, WX, SX, and YL.

509     Drafting of the manuscript: WN, WX, and WZ. Critical revision: WX and WZ. Study conception

510     and design: WX and WZ. Financial support: WX and WZ. All authors read and approved the

511     submitted version of the manuscript. Each author has agreed both be personally accountable for

512     the author's own contributions and to ensure that questions related to the accuracy or integrity of

513     any part of the work, even those in which the author was not personally involved, are appropriately

514     investigated and resolved and that the resolution is documented in the literature.

515

# References

1. Lichtman, E.I. and G. Dotti, *Chimeric antigen receptor T-cells for B-cell malignancies.* Transl Res, 2017. **187**: p. 59-82.

2. Yip, A. and R.M. Webster, *The market for chimeric antigen receptor T cell therapies.* Nat Rev Drug Discov, 2018. **17**(3): p. 161-162.

3. Levine, B.L., et al., *Global Manufacturing of CAR T Cell Therapy.* Mol Ther Methods Clin Dev, 2017. **4**: p. 92-101.

4. Torikai, H. and L.J. Cooper, *Translational Implications for Off-the-shelf Immune Cells Expressing Chimeric Antigen Receptors.* Mol Ther, 2016. **24**(7): p. 1178-86.

5. Roddie, C., et al., *Manufacturing chimeric antigen receptor T cells: issues and challenges.* Cytotherapy, 2019. **21**(3): p. 327-340.

6. Hamieh, M., et al., *CAR T cell trogocytosis and cooperative killing regulate tumour antigen escape.* Nature, 2019. **568**(7750): p. 112-116.

7. https://clinicaltrials.gov/. *AAV.* 2020, january 31; Available from: https://clinicaltrials.gov/ct2/results/browse?term=AAV&brwse=cond_alpha_all.

8. Wang, D., P.W.L. Tai, and G. Gao, *Adeno-associated virus vector as a platform for gene therapy delivery.* Nat Rev Drug Discov, 2019.

9. Grimm, D., et al., *In Vitro and In Vivo Gene Therapy Vector Evolution via Multispecies Interbreeding and Retargeting of Adeno-Associated Viruses.* Journal of Virology, 2008. **82**(12): p. 5887.

10. Wu, X., et al., *Tandem bispecific neutralizing antibody eliminates HIV-1 infection in humanized mice.* J Clin Invest, 2018. **128**(6): p. 2239-2251.

11. Kimura, T., et al., *Production of adeno-associated virus vectors for in vitro and in vivo applications.* Sci Rep, 2019. **9**(1): p. 13601.

12. Kochenderfer, J.N., et al., *Construction and preclinical evaluation of an anti-CD19 chimeric antigen receptor.* J Immunother, 2009. **32**(7): p. 689-702.

13. Chen, Y.H., M.S. Keiser, and B.L. Davidson, *Adeno-Associated Virus Production, Purification, and Titering.* Curr Protoc Mouse Biol, 2018. **8**(4): p. e56.

14. Ellis, B.L., et al., *A survey of ex vivo/in vitro transduction efficiency of mammalian primary cells and cell lines with Nine natural adeno-associated virus (AAV1-9) and one engineered adeno-associated virus serotype.* Virology journal, 2013. **10**: p. 74-74.

15. Ihsan, A.U., et al., *Establishment of a rat model of chronic Prostatitis/Chronic Pelvic Pain Syndrome (CP/CPPS) induced by immunization with a novel peptide T2.* Biomed Pharmacother, 2017. **91**: p. 687-692.

16. Wu, X., et al., *A single-domain antibody inhibits SFTSV and mitigates virus-induced pathogenesis in vivo.* JCI Insight, 2020. **5**(13).

17. Davenport, A.J., et al., *Chimeric antigen receptor T cells form nonclassical and potent immune synapses driving rapid cytotoxicity.* Proc Natl Acad Sci U S A, 2018. **115**(9): p. E2068-e2076.

18. Shu, S.T., et al., *A novel bioluminescent mouse model and effective therapy for adult T-cell leukemia/lymphoma.* Cancer Res, 2007. **67**(24): p. 11859-66.

19. Yu, D., et al., *Targeting Jurkat T Lymphocyte Leukemia Cells by an Engineered Interferon-Alpha Hybrid Molecule.* Cell Physiol Biochem, 2017. **42**(2): p. 519-529.

20. Matsui, W., et al., *Characterization of clonogenic multiple myeloma cells.* Blood, 2004. **103**(6): p. 2332-2336.

562   21.   Grupp, S.A., et al., *Chimeric antigen receptor-modified T cells for acute lymphoid*
563        *leukemia.* N Engl J Med, 2013. **368**(16): p. 1509-18.
564   22.   Mingozzi, F. and K.A. High, *Therapeutic in vivo gene transfer for genetic disease using*
565        *AAV: progress and challenges.* Nature Reviews Genetics, 2011. **12**: p. 341.
566   23.   Brady, J.M., D. Baltimore, and A.B. Balazs, *Antibody gene transfer with adeno-*
567        *associated viral vectors as a method for HIV prevention.* Immunological reviews, 2017.
568        **275**(1): p. 324-333.
569   24.   Wu, Y. and X.-Z. Yu, *Modelling CAR-T therapy in humanized mice.* EBioMedicine,
570        2019. **40**: p. 25-26.
571   25.   Pinz, K., et al., *Preclinical targeting of human T-cell malignancies using CD4-specific*
572        *chimeric antigen receptor (CAR)-engineered T cells.* Leukemia, 2016. **30**(3): p. 701-707.
573   26.   Emu, B., et al., *Phase 3 Study of Ibalizumab for Multidrug-Resistant HIV-1.* N Engl J
574        Med, 2018. **379**(7): p. 645-654.
575   27.   Isaacs, J.D., et al., *Humanized anti-CD4 monoclonal antibody therapy of autoimmune*
576        *and inflammatory disease.* Clinical and experimental immunology, 1997. **110**(2): p. 158-
577        166.
578   28.   van Oosten, B.W., et al., *Treatment of multiple sclerosis with the monoclonal anti-CD4*
579        *antibody cM-T412: results of a randomized, double-blind, placebo-controlled, MR-*
580        *monitored phase II trial.* Neurology, 1997. **49**(2): p. 351-7.
581   29.   Morel, P., et al., *Anti-CD4 monoclonal antibody therapy in severe psoriasis.* J
582        Autoimmun, 1992. **5**(4): p. 465-77.
583   30.   Pohlers, D., et al., *Anti-CD4 monoclonal antibody treatment in acute and early chronic*
584        *antigen-induced arthritis: influence on T helper cell activation.* Clin Exp Immunol, 2004.
585        **135**(3): p. 409-15.
586   31.   Ellis, J., *Silencing and variegation of gammaretrovirus and lentivirus vectors.* Hum Gene
587        Ther, 2005. **16**(11): p. 1241-6.
588   32.   Naso, M.F., et al., *Adeno-Associated Virus (AAV) as a Vector for Gene Therapy.*
589        BioDrugs : clinical immunotherapeutics, biopharmaceuticals and gene therapy, 2017.
590        **31**(4): p. 317-334.
591   33.   Luckheeram, R.V., et al., *CD4$^+$T cells: differentiation and functions.* Clinical &
592        developmental immunology, 2012. **2012**: p. 925135-925135.
593   34.   Ma, G., et al., *Targeting T Cell Malignancies Using CD4CAR T-Cells and Implementing*
594        *a Natural Safety Switch.* Stem Cell Rev Rep, 2019. **15**(3): p. 443-447.
595   35.   Cho, J.H., J.J. Collins, and W.W. Wong, *Universal Chimeric Antigen Receptors for*
596        *Multiplexed and Logical Control of T Cell Responses.* Cell, 2018. **173**(6): p. 1426-
597        1438.e11.
598   36.   Zhao, J., et al., *Universal CARs, universal T cells, and universal CAR T cells.* Journal of
599        hematology & oncology, 2018. **11**(1): p. 132-132.
600   37.   Wang, X. and I. Rivière, *Clinical manufacturing of CAR T cells: foundation of a*
601        *promising therapy.* Molecular Therapy - Oncolytics, 2016. **3**: p. 16015.
602   38.   Qasim, W., et al., *Molecular remission of infant B-ALL after infusion of universal TALEN*
603        *gene-edited CAR T cells.* Sci Transl Med, 2017. **9**(374).
604   39.   Smith, T.T., et al., *In situ programming of leukaemia-specific T cells using synthetic DNA*
605        *nanocarriers.* Nature Nanotechnology, 2017. **12**: p. 813.

606 40.    Pfeiffer, A., et al., *In vivo generation of human CD19-CAR T cells results in B-cell*
607         *depletion and signs of cytokine release syndrome.* EMBO Molecular Medicine, 2018.
608         **10**(11): p. e9158.
609 41.    Klichinsky, M., et al., *Abstract 4575: Chimeric antigen receptor macrophages (CARMA)*
610         *for adoptive cellular immunotherapy of solid tumors.* Cancer Research, 2017. **77**(13
611         Supplement): p. 4575.
612 42.    Romanski, A., et al., *CD19-CAR engineered NK-92 cells are sufficient to overcome NK*
613         *cell resistance in B-cell malignancies.* J Cell Mol Med, 2016. **20**(7): p. 1287-94.
614 43.    Ghosh, A., et al., *Donor CD19 CAR T cells exert potent graft-versus-lymphoma activity*
615         *with diminished graft-versus-host activity.* Nat Med, 2017. **23**(2): p. 242-249.
616 44.    Chan, W.K., et al., *Chimeric antigen receptor-redirected CD45RA-negative T cells have*
617         *potent antileukemia and pathogen memory response without graft-versus-host activity.*
618         Leukemia, 2015. **29**(2): p. 387-95.
619 45.    Depil, S., et al., *'Off-the-shelf' allogeneic CAR T cells: development and challenges.* Nat
620         Rev Drug Discov, 2020.
621 46.    Rossi, A., et al., *Vector uncoating limits adeno-associated viral vector-mediated*
622         *transduction of human dendritic cells and vector immunogenicity.* Sci Rep, 2019. **9**(1): p.
623         3631.
624 47.    Verdera, H.C., K. Kuranda, and F. Mingozzi, *AAV Vector Immunogenicity in Humans: A*
625         *Long Journey to Successful Gene Transfer.* Mol Ther, 2020.
626 48.    Jollé, C., et al., *Development of Efficient AAV2/DJ-Based Viral Vectors to Selectively*
627         *Downregulate the Expression of Neuronal or Astrocytic Target Proteins in the Rat*
628         *Central Nervous System.* 2019. **12**(201).

629
630
631
632
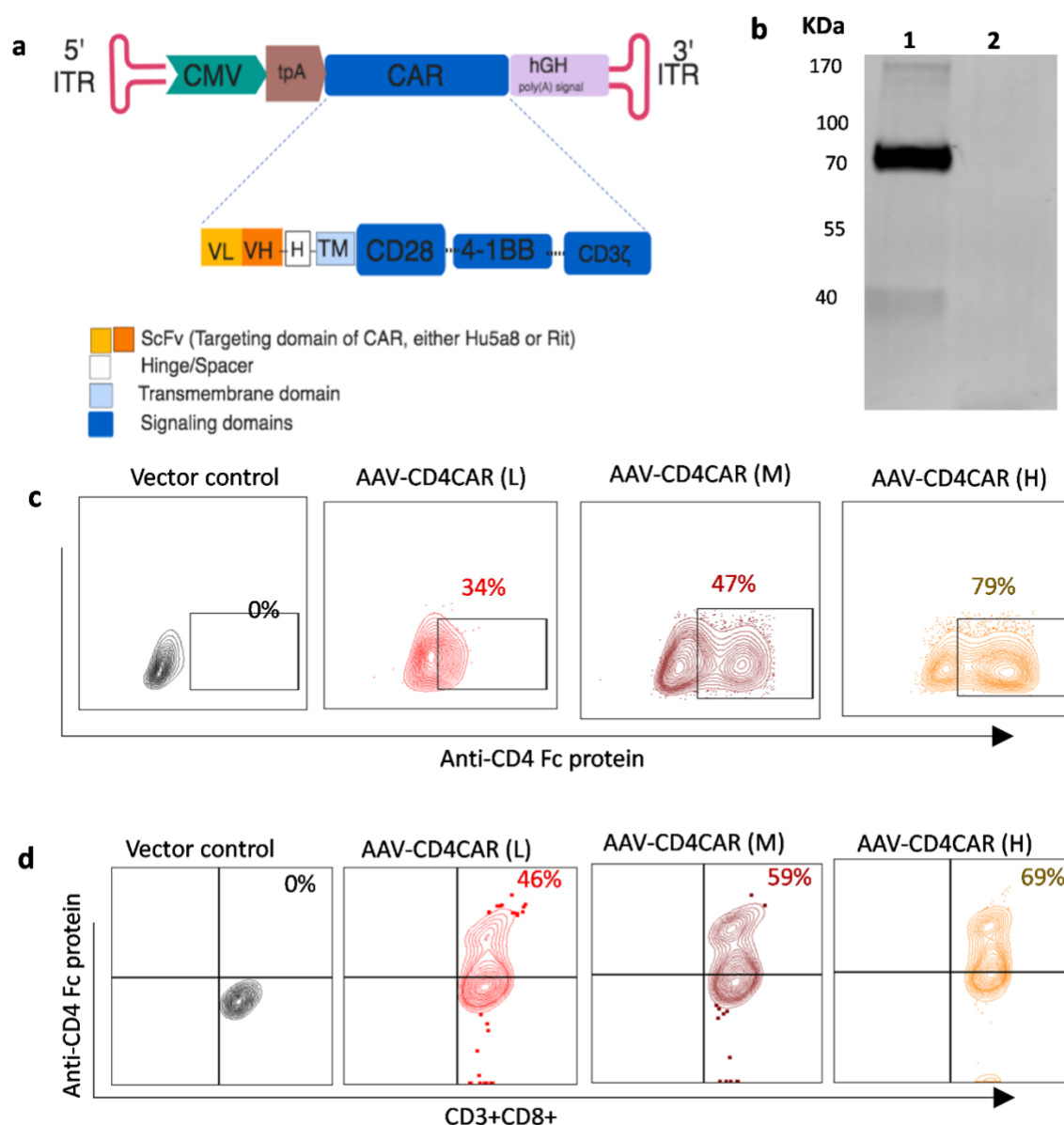633    **Figures and figure legends:**

634
635
636 **Figure 1. AAV-CD4CAR construct and characterization** (**a**) Schematic representation of the
637 AAV encoding CD4CAR or CD20CAR. The third generation of the AAV-CAR contains a leader
638 sequence, the anti-CD4 (Hu5a8) or the anti-CD20 scFv region (Rit), a hinge domain (H), a
639 transmembrane domain (TM) and intracellular signaling domains from the following molecules:
640 CD28 (coactivator), 4-1BB (coactivator), and CD3 zeta. (**b**) HEK293T cells were infected with
641 AAV-CD4CAR (lane 1) and AAV-GFP (lane 2) for Western blot analysis, and at 48 hours post-
642 transduction, they were probed with mouse anti-human CD3 zeta antibody, with the CD4-CAR
643 band observed at the expected size (~75 kDa) and a breakdown product observed at ~37 kDa.

26

644   However, no band was observed for AAV-GFP-transduced cells. **(c)** HEK293T cells were infected
645   with different doses of AAV-CD4CAR. 48 hours post-infection, cells were stained with CD4-rFc
646   protein followed by secondary antibody staining with Alexa Fluor 488-conjugated goat anti-rabbit
647   IgG (H+L). **(d)** AAV-CD4 CAR expression on CD3+CD+8 cells. Activated PBMCs were infected
648   with different doses of AAV-CD4CAR or uninfected (vector control). Forty-eight hours post-
649   infection, cells were stained with CD4-rFc protein for CAR expression, followed by secondary
650   antibody staining with Alexa-Fluor 488-conjugated goat anti-rabbit IgG (H+L). $1x10^4$ AAVs/cell
651   was considered AAV low (L), $1.5x10^4$ AAVs/cell was considered AAV middle (M), and $1x10^5$
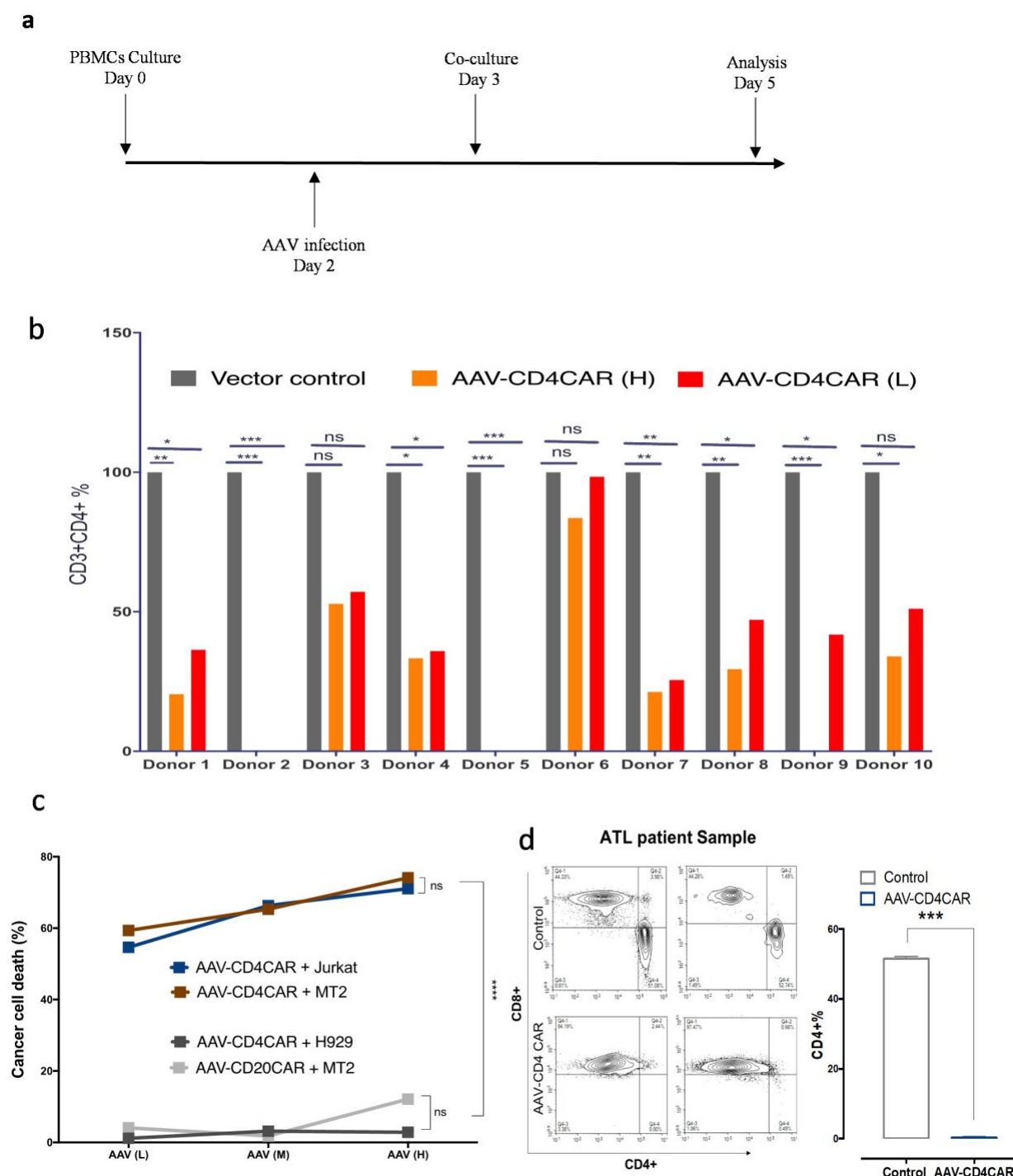652   AAVs/cell was considered AAV high (H).
653
654
655
656

**Figure 2. AAV-CD4CAR induces antitumor activity (a)** Schematic representation showing the *ex vivo* AAV-CAR production and co-culture assays. **(b)** AAV-CD4CAR depleted CD3+CD4+ cells in different donors (n=10) during the course of T cell expansion. Activated PBMCs from each donor were transduced with different doses of AAV-CD4CAR, and Vector control (untransduced). After 48 hours, the cells were analyzed by FACS using anti-human CD4, anti-human CD3, and anti-human CD8 antibodies. The CD3+CD4+ percentage was normalized to the vector control

664     group (which represented 100%), and the CD3+CD4+ percentages of AAV-CD4CAR (H) and
665     AAV-CD4CAR (L) was calculated by the percent difference from the vector control group. A two-
666     way ANOVA multiple comparisons test within each donor was used for statistical analysis. ns, no
667     significance; ***, $P < 0.001$; **, $P < 0.01$; *, $P < 0.05$. **(c)** AAV-CD4CAR T cells were co-cultured
668     with CFSE-stained target cells, 48 hours post-co-culture, cells were stained with 7AAD and
669     analyzed by FACS. Two-way ANOVA with the multiple-comparisons test was used to assess
670     significance, ns, no significance; ****$P < 0.0001$. ***, $P < 0.001$; **, $P < 0.01$; *, $P < 0.05$. **(d)**
671     ATL patient PBMCs were infected with AAV-CD4CAR (H) and with a control vector (samples
672     were duplicated). 48 hours post-transduction, cells were analyzed by FACS for CD3+CD4+
673     depletion. An unpaired two-tailed t-test was used to calculate the significance of the difference.
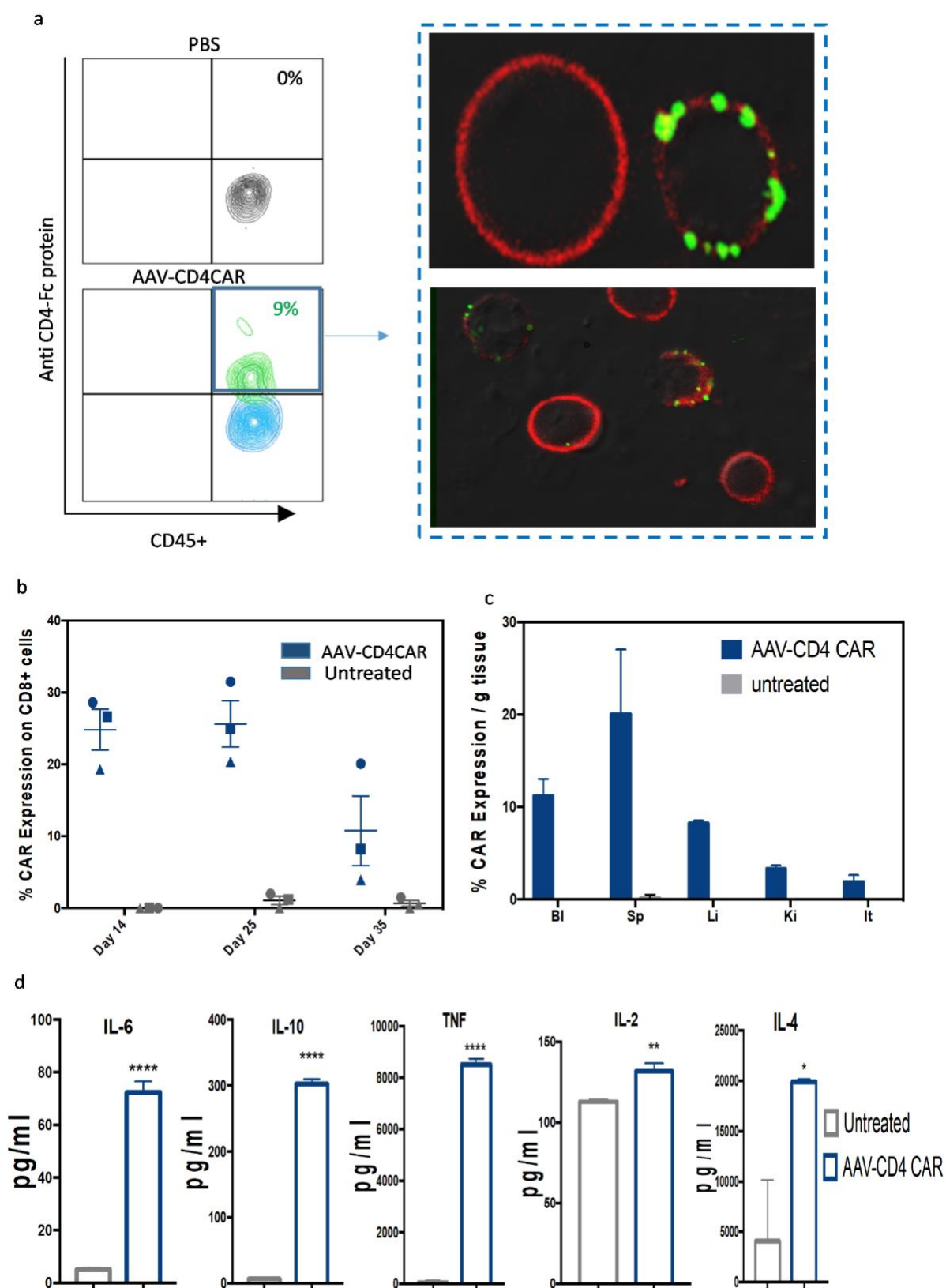674     AAV-CD4CAR vs vector control, ***, $P<0.0001$.
675
676
677

678

679  **Figure 3. AAV-CD4CAR reprograms immune cells and generates *in vivo* tumor-specific**
680  **AAV-CD4CAR T cells. (a)** Representative flow cytometry results showing the expression of
681  AAV-CD4CAR on CD45+ cells 48 hours after infusing a single dose of 1 x $10^{11}$ AAV-CD4CAR
682  into NCG-HuPBL mice (n=3). The right panel shows the confocal imaging of CD45+ cells
683  expressing AAV-CD4CAR expression. The red shows the cellular membrane, whereas the green
684  dots represent AAV-CD4CAR expression on the cell. **(b)** A total of 1 x $10^{11}$ AAVs carrying the
685  CD4CAR gene were injected into mice (n=3), and AAV-CD4CAR expression was demonstrated
686  by FACS at the indicated time. Distinct symbols represent different donor PBMCs used for the
687  development of the HuNCG mouse model. All data are shown as the mean ± s.e.m. with error bars
688  on the graph. **(c)** Graphical representation of the biodistribution of AAV-CD4CAR T cells in
689  various tissues (n=3). Bl, blood; Sp, spleen; Li, liver; Lu, lung; It, intestine; Ki, kidney. Cells
690  isolated from the spleen, liver, kidney, blood, and intestine were analyzed by flow cytometry for
691  AAV-CD4CAR expression on CD8+ cells. All data are shown as the mean ± s.e.m. with error bars
692  on the graph. **(d)** Graphical representation of different cytokines detected in the plasma of tumor-
693  bearing ATL NCG-HuPBL mice (n=3), at 2 weeks after AAV injection. Cytokines were detected
694  through FACS by using the BD Cytometric Beads Array Human Th1/Th2 Cytokine Kit. An
695  unpaired two-tailed t-test was used for analysis. ns, no significance; ****$P < 0.0001$. ***, $P < $
696  $0.001$; **, $P < 0.01$; *, $P < 0.05$.
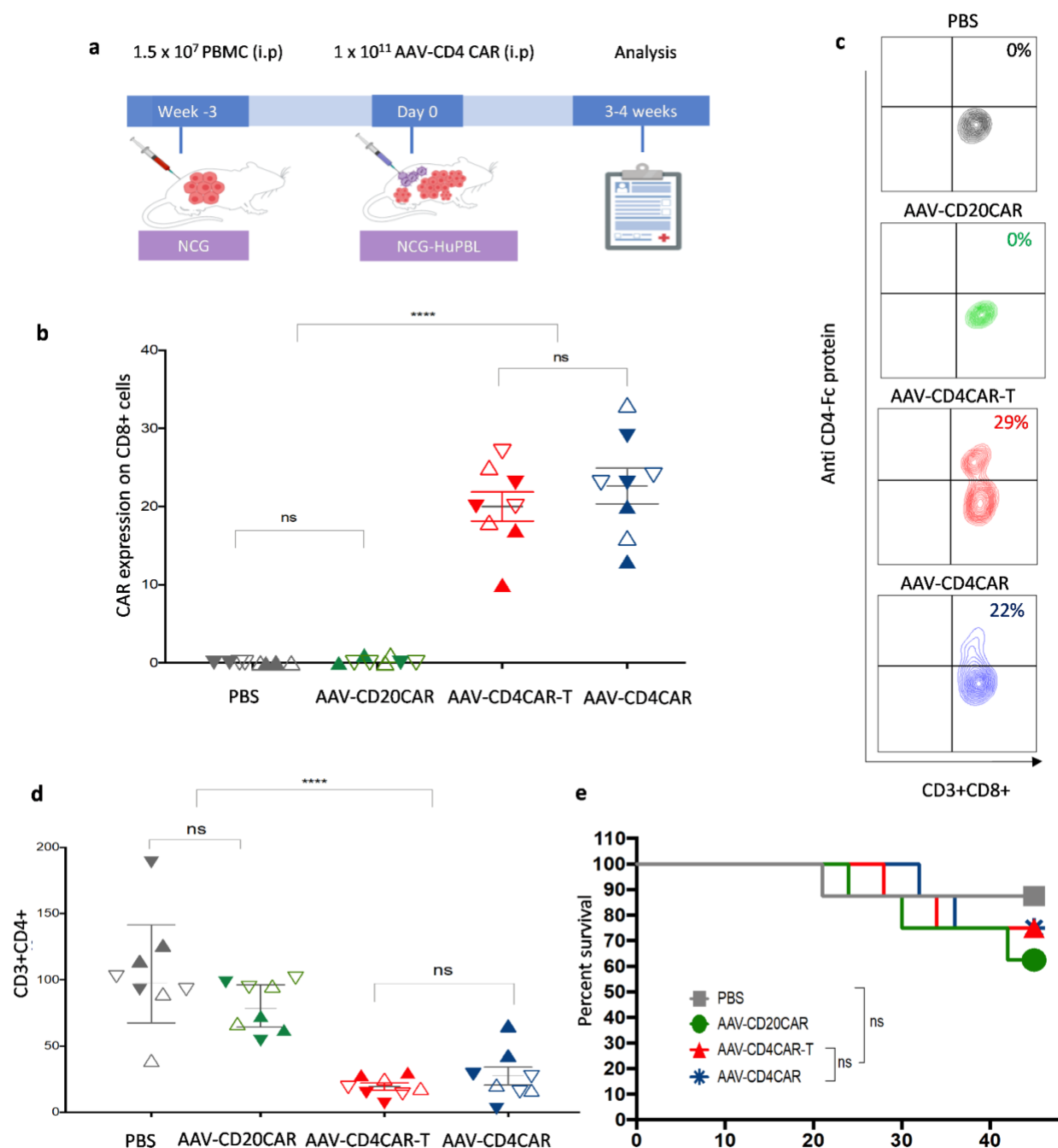697
698
699
700

31

**Figure 4. Functional characterization and comparative study of *in vivo*-generated AAV-CD4CAR T cells. (a)** Schematic representation showing the development of NCG-HuPBL mouse model and experimental design. **(b)** Graphical representation of CAR expression using the CD4-Fc protein in different groups one week after the treatment. The NCG-HuPBL mouse model was developed by using PBMCs from four different healthy donors. Successful NCG-HuPBL mice were randomly divided into four groups, and each group contained eight mice from four different donors. Distinct symbols are used to differentiate the NCG-HuPBL mice engrafted with different donor PBMCs. The treatment regimen was started at day 0 as specified for each group in the main

32

711 text. Blood was collected from each mouse and evaluated for CAR expression through FACS.
712 Data were analyzed by using two-way ANOVA for multiple comparisons. ****$P < 0.0001$, ns,
713 No significance. **(c)** Exemplary counter plot showing the CAR expression of a single mouse
714 sample from each group. **(d)** Graphical representation of the normalized CD3+CD4+ percentage
715 documented after 14 days of treatment. Two weeks following the treatment, peripheral blood was
716 collected from each mouse and analyzed for the CD3+CD4+ population through FACS. The
717 CD3+CD4+ cell percentage of each mouse was normalized to 100% at day 0. The CD3+CD4+
718 percentage at week 2 for each mouse was calculated by the percent difference from the
719 corresponding mice at day 0. Data were analyzed by using two-way ANOVA for multiple
720 comparisons. ****$P < 0.0001$, ns,   No significance.   **(e)** Kaplan–Meier curves for percent survival
721 of mice used in (A and B). Percent survival between the groups was analyzed by the log-rank test;
722 $P < 0.05$ was considered significant.
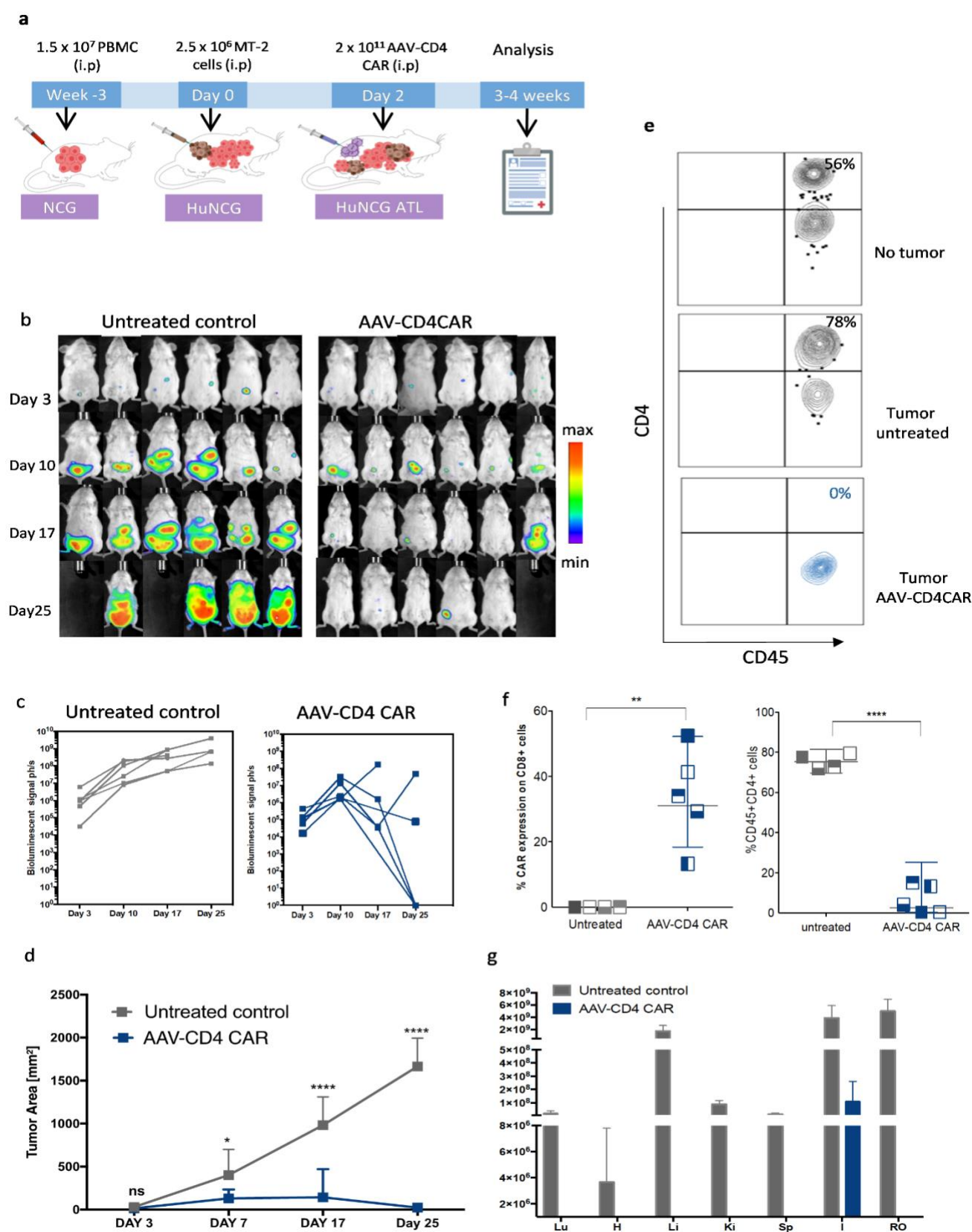723
724

725

34

726

727  **Figure 5. *In vivo*-generated AAV-CD4CAR T cells mediated antitumor activity. (a)** Schematic
728  representation showing the development of HuNCG ATL mouse model and experimental design.
729  **(b)** Sequential *in vivo* imaging of luciferase-expressing MT2 ATL cells injected into NCG-HuPBL
730  mice. Following AAV or PBS (untreated) injection, mice were imaged the next day, followed by
731  *in vivo* imaging at different time points as specified in the figure. Blank images represent dead
732  mice. **(c)** Bioluminescent intensity (p/sec) of mice shown in B. Each line represents one mouse.
733  **(d)** Mean tumor area of AAV-CD4CAR-treated mice and untreated mice. Two-way ANOVA with
734  multiple comparisons was used to analyze the mean tumor area. ns, no significance，*P<0.05,
735  ****P<0.0001.Data are presented as the mean ± SEM. **(e)** Exemplary counterplot of FACS
736  analysis showing the CD45+CD4+ percentage in NCG-HuPBL mice (no tumor, no treatment),
737  untreated NCG-HuPBL tumor challenge mouse and AAV-CD4CAR-treated NCG-HuPBL tumor
738  challenge mouse at the end of the study. **(f)** The CD45+CD4+ percentage and AAV-CD4 CAR
739  expression of the mice in B. Blood was collected from each mouse at the end of the study and
740  analyzed by FACS for the CD45+CD4+ percentage and CAR expression on CD3+CD8+ cells. An
741  unpaired t-test was used to analyze the data. **P<0.001, ****P<0.0001. **(g)** Graphical
742  representation of tumor distribution in different organs. Two mice from each group were selected
743  and sacrificed at the end of the study (Supplemental Figure 4). Organs from dissected mice were
744  imaged immediately after sacrifice. The bioluminescent intensity (pH/s) of each organ was
745  quantified and presented as the mean ± SEM. Lu, Lung; H, Heart; Li, Liver; Ki, Kidneys; Sp,
746  spleen; I, Large and small intestine; RO, Reproductive organs.

747